Polyaromatic Assembly Mechanisms and Structure Selection in Carbon Materials

Robert Hurt,*,† Gernot Krammer,‡ Gregory Crawford,† Kengqing Jian,† and Christopher Rulison§

Division of Engineering, Brown University, Providence, Rhode Island 02912, Technical University of Graz, Graz, Austria, and KRÜSS USA, Charlotte, North Carolina 28270

Received April 1, 2002. Revised Manuscript Received September 24, 2002

This article reports on the interfacial behavior of large liquid-phase polycyclic aromatic hydrocarbons in pitches that are common precursors to carbon materials. Experiments were conducted to identify preferred angles of molecular orientation ("surface anchoring" states) and to measure contact angles on a variety of well-characterized substrates. The results show that the large disklike polyaromatic molecules exhibit anomalously weak noncovalent interactions with a variety of surfaces, a fact that we attribute to inhibition of dispersion forces due to geometric mismatch at the interface. It is further found that large polyaromatics prefer edge-on molecular orientation at most interfaces, a configuration that preserves internal aromatic $\pi-\pi$ bonds at the expense of inhibited $\pi-$surface bonds. A theory of $\pi-\pi$ bond preservation is proposed to explain many aspects of wetting, adsorption, anchoring, and supramolecular assembly in this important class of compounds, including the formation mechanism for the classic bipolar Brooks−Taylor mesocarbon spheres. The results are used to discuss the mechanisms of structure selection in carbon materials prepared at high and low temperatures. The results are also used to demonstrate a new approach for molecular engineering of carbon that employs anchoring templates to synthesize new materials with preprogrammed patterns of graphene layer orientation.

Introduction

Nanotubes, fullerenes, carbon black, glassy carbon, and many other carbon forms have surfaces that exhibit the essential properties of graphene basal planes,[1−3] including chemical inertness that causes weak bonding in assemblies and composites and limits options for covalent functionalization.[4] An alternative carbon form with inverted, "open" crystal structure and accessible reactive graphene edge sites is found in nature,[5−7] and in some carbons prepared by controlled heat treatment of condensed phase precursors that pass through a fluid state[6−10] (see Figure 1). The fundamental molecular assembly principles that govern structure selection in these carbon forms are poorly understood, although it is clear that the inverted form involves discotic polyaromatic compounds (Figure 2) as liquid crystalline intermediate phases.[6−10]

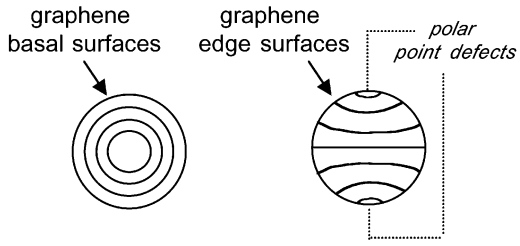

Figure 1. Two classes of contrasting crystal symmetries in carbon bodies. Lines are drawn parallel to aromatic planes or graphene layers. Left: concentric symmetry of "closed" carbon forms: carbon black, nested fullerenes, and multiwall nanotubes in cross section. Right: bipolar symmetry of Brooks−Taylor carbon spheres with "open" crystal structure, formed from condensed phase precursors that pass through a fluid state during carbonization.[5−7]

Polycyclic aromatic hydrocarbons (PAHs) are common chemical intermediates in the formation of carbon, as they lie along the minimum free energy pathway in C/H space between organic matter and the atmospheric-pressure thermodynamic end-state, graphite. PAHs are ubiquitous in nature where they are of special interest as pollutants in the atmosphere and soil;[11,12] as biologically active compounds that form carcinogen-DNA adducts[13,14] and exert complex effects on the immune

* Corresponding author. Tel: 401 863 2685. Fax: 401 863 1157. E-mail: Robert_Hurt@brown.edu.
† Brown University.
‡ Technical University of Graz.
§ KRÜSS USA.

(1) Kroto, H. W.; Heath, J. R.; O'Brian, S. C.; Curl, R. F.; Smalley, R. E. *Nature* **1985**, *318*, 162.
(2) Iijima, S. *Nature* **1991**, *354*, 56.
(3) Oberlin, A. In *Chemistry and Physics of Carbon, Vol. 22*; Marcel Dekker: New York, 1989; Chapter 1.
(4) Chen R. J.; Zhang, Y.; Wang, D.; Dai, H. *J. Am. Chem. Soc.* **2001**, *123*, 3838.
(5) Brooks, J. D.; Taylor G. H. *Nature* **1965**, *697*, 206.
(6) Brooks, J. D.; Taylor, G. H. *Carbon* **1965**, *3*, 185.
(7) Hurt, R. H.; Chen, Z.-Y. *Phys. Today* **2000**, *53* (3), 39.
(8) Marsh, H.; Walker, P. J., Jr. In *Chemistry and Physics of Carbon, Vol 15*, Marcel Dekker: New York, 1979.
(9) Rand, B. In *Handbook of Composites, Strong Fibers, Vol. 1*; Elsevier: Amsterdam, 1985.
(10) Dubois, J.; Agache, C.; White, J. L. *Metallography* **1970**, *3*, 337.
(11) Dimashki, M.; Lim, L. H.; Harrison, R. M.; Harrad, S. *Environ. Sci. Technol.* **2001**, *35*, 2264.
(12) Arzayus, K. M.; Dickhut, R. M.; Canuel, E. A. *Environ. Sci. Technol.* **2001**, *35*, 2178.

10.1021/cm020310b CCC: $22.00
Published on Web 10/31/2002

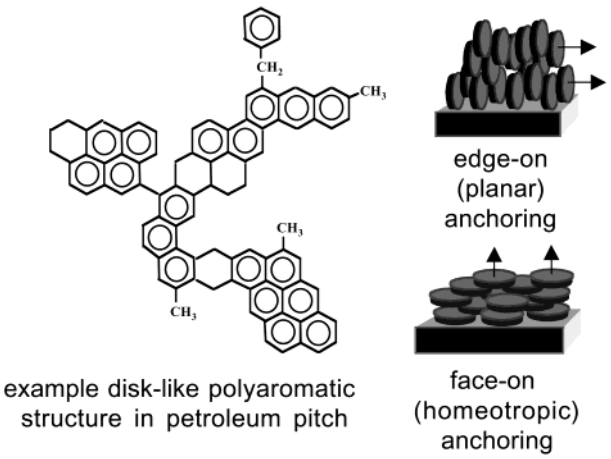

Figure 2. Left: Example of disklike polyaromatic structure in petroleum pitch. Right: Sketch of the discotic nematic phase and two surface anchoring states. The designations "edge-on" and "face-on" refer to the orientation of the molecular planes, whereas the equivalent terms commonly used in the liquid crystal literature, "planar" and "homeotropic" refer to the orientation of the director (mean of orientational molecular unit vectors) which lies normal to the molecular plane.

system;[15] as components in the interstellar medium;[16] and as components in petroleum that cause harmful deposits in processing equipment.[17] In technology PAHs find use as liquid crystalline cores;[18−20] as optoelectronic devices including diodes and organic molecular thin films;[21−26] as organic superconductors;[27] as feedstocks for advanced carbon materials[9,28,29]; and as enabling elements of nanotechnology used for molecular recognition,[30] as molecular wires,[25] or as coupling agents for sidewall functionalization of nanotubes.[4] Soft interactions of PAHs and their noncovalent assembly mechanisms are important in many of these applications.

Among naturally occurring polyaromatics are those of high molecular weight (300−2000 Daltons), which can be disklike or platelike (see Figure 2) and are known to form an ordered, liquid crystalline (LC) phase known as carbonaceous mesophase.[7−10] High molecular weight PAHs in the form of pitches derived from heat soaking and/or extraction of petroleum fractions[31] or coal tar, or from the polymerization of naphthalene[28] are promising feedstocks for advanced carbon materials, including battery electrodes, graphite foams for thermal management applications, and high-modulus carbon fibers.[9,28,29] Despite their technological importance, our fundamental understanding of *very* large PAH behavior (>700 Daltons) is limited because of their availability only as complex mixtures.[7] Perversely, the mixture form of these materials is essential to the observation of their liquid crystalline behavior—in the pure state, large, regular, unsubstituted polyaromatics are insoluble,[32,7] nonvolatile,[17] and form high-melting solid phases that mask the discotic liquid crystalline behavior.[7] Any meaningful research on these important mesophase materials *must* therefore employ them in their naturally occurring multicomponent form. The primary LC phase is the discotic nematic, with long-range orientational order, but no long-rang positional order (Figure 2). Some local columnar stacking is observed,[3] but the wide variety of molecular sizes and shapes within carbonaceous mesophase prevents the formation of a true columnar phase with the required long-range positional order.

During heating of polyaromatic liquids, anisotropic liquid droplets of higher molecular mean weight and/or size appear and grow within the continuous isotropic liquid phase. Several molecular structures have been reported for these spherical droplets, but the most common is the classical Brooks−Taylor structure with bipolar symmetry (Figure 1) first reported in *Nature*[5] in 1965. A possible explanation for the origin of the particular bipolar structure is a strong preference for edge-on molecular orientation at the phase boundary. The general phenomenon of interfacial molecular orientation in liquid crystal systems is referred to as "surface anchoring"[19,20,33−37] and is fundamental to liquid crystal science and technology. Surface anchoring states are determined by a complex interplay of the molecular structure of the LC molecules, the substrate chemistry, the substrate topology, and possible surface texture induced by directional rubbing.[19,20,33−37] Because of this complexity, anchoring states must be determined experimentally for the LC/substrate pair of interest. Despite the technological importance of carbonaceous mesophase, there are no systematic experimental studies of its anchoring states in the archival literature.

There have been several anchoring studies for pure discotic LCs,[19,20,38,39] but these materials differ signifi-

(13) Perlow, R. A.; Broyde, S. *J. Mol. Biol.* **2001**, *309*, 519.
(14) Lin, C. H.; Huang, X. W.; Kolbanovskii, A.; Hingerty, B. E.; Amin, S.; Broyde, S.; Gecintov, N. E.; Patel, D. J. *J. Mol. Biol.* **2001**, *306*, 1059.
(15) Burchiel, S. W.; Luster, M. I. *Clin. Immunol.* **2001**, *98*, 2.
(16) Salama, F. *J. Mol. Struct.* **2001**, *563*, 19.
(17) Qian, K.; Edwards, K. E.; Siskin, M. *Energy Fuels* **2001**, *15*, 949.
(18) Brown, S. P.; Schnell, I.; Didrich, B.; Müllen, K.; Spiess, H. W. *J. Am. Chem. Soc.* **1999**, *121*, 6712.
(19) Perova, T. S.; Vij, J. K.; Kocot, A. *Europhys. Lett.* **1998**, *44* (2), 198−204.
(20) Orgasinska, B.; Perova, T. S.; Merkel, K.; Kocot, A.; Vij, J. K. *Mater. Sci. Eng.* **1999**, *C8*−*9*, 283−289.
(21) Schön, J. H.; Kloc, Ch.; Bucher, E.; Batlogg, B. *Nature* **2000**, *403*, 408.
(22) Meyer zu Heringdorf, F. J.; Reuter, M. C.; Tromp, R. M. *Nature* **2001**, *412*, 517.
(23) Schmitz-Hübsch, A.; Sellam, F.; Staub, R.; Rörker, M.; Fritz, T.; Kübel, C.; Müllen, K.; Leo, K. *Surf. Sci.* **2000**, *445*, 358.
(24) England, C. D.; Collins, G. E.; Schuerlein, T. J.; Armstrong, N. R. *Langmuir* **1994**, *10*, 2748−2756.
(25) Keil, M.; Samoir, P.; dos Santos, D. A.; Kugler, T.; Stafström, S.; Brand, J. D.; Müllen, K.; Bredas, J. L.; Rabe, J. P.; Salaneck, W. R. *J. Phys. Chem. B.* **2000**, *104*, 3967−3975.
(26) Hooks, D. E.; Fritz, T.; Ward, M. D. *Adv. Mater.* **2001**, *13* (4), 227−241.
(27) Schön, J. H.; Kloc, Ch.; Batlogg, B. *Nature* **2000**, *406*, 702.
(28) Mochida I.; Korai, Y.; Ku C. H.; Watanabe, F.; Sakai Y. *Carbon* **2000**, *38*, 305.
(29) McHugh, J. J.; Edie, D. D. *Carbon* **1996**, *34*, (11), 1315.
(30) Hunter, C. A.; Sanders, J. K. M. *J. Am. Chem. Soc.* **1990**, *112*, (14) 5525.
(31) Dauche, F. M.; Bolanos, G.; Blasig, A.; Thies, M. C. *Carbon* **1998**, *36*, 6(7−8), 953.
(32) Iyer, V. S.; Yoshimura, K.; Enkelmann, V.; Epsch, R.; Rabe, J. P.; Müllen, K. *Angew. Chem., Int. Ed.* **1998**, *37*, 2696.
(33) Uchida T.; Seki, H. In *Liquid Crystals Applications and Uses, Vol. 3*; Bahadur, B., Ed.; World Scientific: Singapore, 1992.
(34) Creagh, L. T.; Kmetz, A. R. *Mol. Cryst. Liq. Cryst.* **1973**, *24*, 59−68.
(35) Sonin, A. A. *The Surface Physics of Liquid Crystals*; Gordon and Breach Publishers: Luxembourg, 1995.
(36) Vauchier, C.; Zann, A.; Barny, P. L.; Dubois, J. C.; Billard, J. *Mol. Cryst. Liq. Cryst.* **1981**, *66*, 103.
(37) Levelut, A. M.; Hardouin F.; Gasparoux, H.; Destratde, C.; Tinh, N. H. *J. Phys.* **1981**, *42*, 147.
(38) Owens, D. K.; Wendt, R. C. *J. Appl. Polym. Sci.* **1969**, *13*, 1741.
(39) Schultz, J. *J. Colloid Interface Sci.* **1977**, *59*, 272.

cantly from the polyaromatics in pitch, as the former possess multiple aliphatic or alkoxy side chains of significant length, and tend to form columnar rather than nematic phases. Useful insights into PAH surface molecular orientation can be drawn from the literature on molecular thin films,[22−26] including studies of pentacene on Si(001)[22,] coronene on MoS_2[newB],[24] and hexa-peri-hexabenzocoronene on highly oriented pyrolytic graphite (HOPG),[23,25] $MoS_2$25, oxidized silicon-(001),[25] and polycrystalline gold.[25] These pure polyaromatics, however, are not necessarily reliable models for the very large discotic mesogens in pitch. For example, coronene and hexa-peri-hexabenzocoronene are regular, rotationally symmetric molecules whose face-to-face dimers are shifted in response to opposing quadropoles, and this interaction gives rise to a titled "herringbone" structure in the bulk crystal. This preferred herringbone structure and its mismatch with the graphite lattice has been cited by Keil et al.[25] as a likely cause for the formation of edge-on needlelike clusters in annealed films on HOPG. The larger, irregular polyaromatic mixtures of interest in the present article do not exhibit herringbone structures, and indeed we find a preferred face-on molecular orientation for these materials on HOPG, even upon extended annealing.

Here we have conducted a basic investigation of the surface anchoring states of the large polyaromatics in carbonaceous mesophase on a variety of interfaces, complemented by experiments on mesophase pitch wetting behavior that provides additional information on interfacial interactions. The results are used to understand the liquid phase assembly mechanisms of very large PAHs and to demonstrate a new method for molecular engineering of carbon materials using surface anchoring templates.

Materials and Experimental Procedures

AR mesophase pitch (Mitsubishi Gas Chemical, HP grade) was used as a model high-molecular-weight polyaromatic liquid. It is synthesized by polymerization of naphthalene to a distribution of oligomers with molecular weights from 200 to 1400 Daltons with a peak of the molecular weight distribution at about 600 Daltons.[28] AR mesophase has a C/H atomic ratio of 1.6, and softens at 280−350 °C to form a homogeneous discotic liquid crystalline phase. Several anchoring experiments were also carried out with a petroleum mesophase pitch fraction supplied by Professor M. Thies at Clemson University. Several wetting experiments were carried out with a single-component, four-ring polyaromatic compound, dimethylbenz-[*a*]anthracene, $C_{20}H_{16}$. For comparison, selected wetting experiments were also carried out with Ashland A240 isotropic petroleum pitch, which is rich in polyaromatics but softens at lower temperature and does not form a liquid crystalline phase. The oxygen content of polyaromatic liquids was measured directly by the Unterzaucher technique at Huffman Analytical Labs, Golden, CO. Liquid surface tensions were measured by the pendent drop method in nitrogen atmosphere at 325 °C for AR, and at 150 °C for $C_{20}H_{16}$ and Ashland A240 pitch, using the Kruss DSA10 drop shape analysis system for image acquisition and processing.

Surface anchoring states (see Figure 2) were determined experimentally by coating polyaromatic liquid crystalline films onto transparent, removable, or etchable substrates at 325 °C, just above the softening or melting point, followed by quenching to room temperature and direct microscopic examination of the interface (see Figure 3). Under these conditions the pitch solidifies after only 20−50 °C of cooling to form stable structures that preserve the LC anchoring states. For glass, quartz, sapphire, ITO, and polytretrafluorethylene (PTFE) thin films the anchoring states were determined by direct imaging through the transparent substrates, whereas for highly oriented pyrolytic graphite (HOPG) the substrate was removed physically by peeling, and the metal films were etched with HCl prior to microscopic examination. Cross sections of selected samples were prepared by vacuum impregnation of epoxy followed by grinding and fine polishing. Edge-on and face-on anchoring states were identified through the presence or absence of optical anisotropy (LC texture) at the interface, respectively (see Figure 3), and molecular orientations in the interfacial plane were determined by microscopic inspection under crossed polars, with and without a $^1/_2$-wave retarder plate, by the standard technique involving color calibration of the optical system using natural flake Ticonderoga graphite with known orientation of graphene layers (see Figure 3).

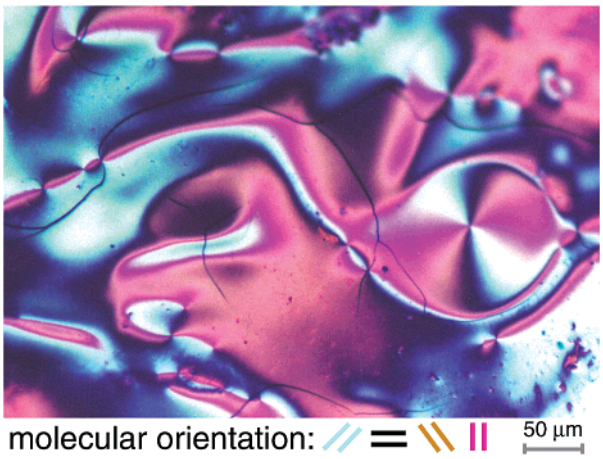

Figure 3. Polarized light micrograph of polyaromatic (AR-mesophase) free surface (gas interface). The classical nematic liquid crystal texture with pronounced optical anisotropy indicates edge-on molecular orientation, either strictly perpendicular to the surface or tilted, with random orientation of domains within the interfacial plane ("planar heterogeneous" in liquid crystal terminology). This imaging mode using crossed polarizing filters with $^1/_2$-wave retarder plate, which reveals the in-plane molecular orientation of the edge-on disks after calibration with natural Ticonderoga flake graphite (see key).

To better understand polyaromatic/substrate interfacial interactions, contact angles between polyaromatic liquids and various solid surfaces previously exposed to ambient air were measured at 325 °C (for AR) or 150 °C (for A240 and $C_{20}H_{16}$) in nitrogen purge also using the DSA10 image acquisition system. The same set of solid surfaces were characterized for surface energy and its dispersive and polar components by application of the standard Owens−Wendt theory[38] to contact angles of standard reference liquids (diiodomethane and water) measured by the Schultz technique[39]. [The Schultz technique is a modification of the standard wetting experiment designed to accommodate high-energy surfaces. It involves examination of the contact angle between a standard liquid (here diiodomethane, water, or chloroform) and a test substrate at the three-phase boundary with a third standard liquid (hexane) whose presence prevents the total wetting of the high energy surfaces and associated loss of interfacial information.]

Contact angles were also measured for chloroform in order to allow the substrates to be further characterized by the van Oss theory,[40] a three-component theory that partitions the total surface energy into dispersive, acidic, and basic components, and requires data on three standard liquids. The sample sets for wetting and anchoring are not identical, but do overlap greatly which allows exploration of relationships between the two phenomena.

(40) Van Oss, C. J.; Good, R. J.; Chaudhury, M. K. *J. Colloid Interface Sci.* **1986**, *376*, 111.

Table 1. Anchoring States for Polyaromatics[a] at Various Interfaces

substrate	dominant anchoring state[b]
aluminum	edge-on
alumina	edge-on
borosilicate glass	edge-on
rubbed boro. glass	edge-on
copper	edge-on
graphite basal plane	
HOPG	face-on (homeotropic)
flexible sheet	face-on (homeotropic)
indium tin oxide	edge-on
muscovite mica	face-on (homeotropic)
PTFE	edge-on
quartz	edge-on
sapphire	edge-on

[a] Primary material: AR-mesophase pitch (HP grade). Several experiments with a petroleum mesophase pitch gave the same results as for AR: edge-on anchoring on borosilicate glass and at the gas interface, and face-on anchoring on HOPG. [b] All edge-on states are planar heterogeneous.

Results

Figure 3 is an optical micrograph of a free surface of the polyaromatic AR-mesophase pitch (i.e., liquid/gas interface), which shows pronounced optical anisotropy and classic nematic liquid crystal texture. The anisotropy indicates edge-on orientation ("planar heterogeneous" anchoring) with the discotic molecules either strictly perpendicular to the interface or tilted. The edge-on anchoring state at the free surface was confirmed by optical examination of polished cross sections, though in some cases the edge-on films were near the limit of optical resolution. For this reason we find that direct examination of the interface is a more reliable general technique for determining anchoring states than examination of cross-sections. Similar edge-on orientation is observed on most of the substrates examined (see Table 1). In-plane orientations of the edge-on domains were always random, and even directional rubbing of the glass substrates with a felt cloth or with an abrasive paper could not achieve a preferred in-plane orientation of this discotic phase as it does for some other LC systems.[35] Face-on anchoring is observed only for mica and for the graphite basal plane, both for HOPG and a flexible graphite sheet. These substrates produce a polyaromatic liquid interface that is featureless and directionally invariant (shown as dark intergrid regions in Figure 5), indicating strict face-on ("homeotropic") orientation of the disklike molecules. The pitch/mica interface showed some patches of edge-on orientation, indicating either a weaker face-on preference on mica relative to graphite, or to a greater abundance of surface defects.

Measured values of surface tension for three polyaromatic liquids and their contact angles on various substrates are reported in Table 2. The table also gives the surface energies and their polar and dispersive components of the bare solid surfaces determined in separate wetting experiments with standard reference liquids. Note that the graphite basal plane shows a small polar component, which may be due to $\pi-$H bond formation with the standard probe liquid, water. An anomalous feature in these data is the increase in contact angle with increasing surface energy in the range 65−78 mJ/m^2, implying that wetting is more favorable on lower energy surfaces in this range. This is opposite to the trend observed with most liquids, and is in conflict with the general practice of surface treatment in composite materials, where surface energy is intentionally enhanced to promote wetting and interfacial adhesion.

Analysis and Discussion

The observation of edge-on anchoring at the free surface is in agreement with the previous observation of White,[41] and indicates by trivial application of the principle of free energy minimization that the edge-on surfaces in carbonaceous mesophase have a lower surface free energy than face-on (basal) surfaces. Note that this relation is the inverse of that seen for crystalline graphite, where the edge planes typically have higher energies than basal planes, likely due to unsatisfied valencies and oxide groups on graphite edge-sites. As a result graphite edge-plane surfaces are capable of high-energy covalent and/or polar interactions, in contrast to the hydrogen-capped polyaromatic edges in

Table 2. Solid Surface Energies and Polyaromatic Liquid Surface Tensions and Contact Angles

polyaromatic liquid surface tensions

AR-mesophase[a]	27.0 mJ/m^2
$C_{20}H_{16}$[c]	26.0 mJ/m^2
A240 pitch[d]	32.5 mJ/m^2

surface properties and contact angles

liquid/substrate	surface energy[b]	dispersive part[b]	polar part[b]	polyarom. contact angle degrees	inhibition factor F_I	effect. solid dispersive energy, $F_I^2\gamma_s^d$
AR[a]/PTFE	18	18	0	66.5	0.86	13.3
AR[a]/borosilic. glass	67.5	33.9	33.6	26.8	0.84	23.9
AR[a]/aluminum	72.4	34.6	37.8	35.9	0.80	22.1
AR[a]/iron	72.5	33.8	38.7	37.0	0.80	21.6
AR[a]/bisque alumina	78.0	33.1	44.9	40.6	0.79	20.6
AR[a]/HOPG basal	40.5	32.7	7.9	17.2	0.89[e]	25.9
AR[a]/mica	60.9	31.3	29.6	26.9	0.88[e]	24.1
$C_{20}H_{16}$[c]/PTFE	18	18	0	55.4	0.94	16.0
A240/borosil. glass	67.5	33.9	33.6	42.1	0.85	24.5
A240/PTFE	18	18	0	68.0	0.92	15.4

[a] HP grade at 325 °C. [b] Solid surface energies and components, mJ/m^2. [c] Dimethylbenz[*a*]anthracene at 150 °C. [d] A240 isotropic petroleum pitch at 150 °C. [e] Approximate value only, because wetting occurs with an anchoring state (face-on) that is different from the anchoring state during surface tension measurement (edge-on). The value of F_I given is accurate in the limiting case when the anisotropic component of surface tension is small.

mesophase, which are capable of only dispersive interactions. On substrates there is a strong tendency toward edge-on anchoring, with the lamellar materials graphite (basal plane) and mica being the notable exceptions.

Relevant data in the pitch literature are few, but include observations of face-on orientation on various carbon materials[42] and a conference report of edge-on orientation on a variety of ceramic materials,[43] consistent with the trends observed here. The known pure discotic LCs are generally unreliable models for the polyaromatics of interest here because their polyaromatic cores are highly substitituted with aliphatic or alkoxy chains. Nevertheless the pure discotics show similar trends, with the most common anchoring state reported to be edge-on.[19] Examples are hexapentyloxytriphenylene on untreated Si, CaF2, ZnSe, and ZnS[19,20] and triphenylene derivatives on glass[20,37] all of which are edge-on. Face-on orientation has been reported on the lamellar materials muscovite and apophylite.[36] Relevant observations from the molecular thin film literature indicate face-on configuration for single pentacene molecules on silicon(001), but edge-on orientation for multimolecular islands, suggesting the greater importance of intermolecular interactions among pentacene molecules relative to pentacene/substrate interactions.[22] Face-on orientation on HOPG has been reported for coronene[24] and hexa-peri-bonzocoronene,[23] at least for monolayer and submonolayer coverage.

The largest PAH studied, hexa-peri-hexabenzocoronene, adsorbs face-on on two atomically flat layered materials (HOPG, MoS_2), and edge-on on the atomically rough oxidized silicon(001) and polycrystalline gold, similar to the trends reported here.[25] The film structure of hexa-peri-hexabenzocoronene on HOPG was not stable during annealing at 425 K, however, and converted to edge-on needlelike domains, which has been attributed to intermolecular interactions that favor titled herringbone structures, which are mismatched to the atomically flat HOPG surface.[25] In general, surface molecular orientation in pitch anchoring, pure discotic anchoring, and PAH epitaxial deposition are all governed by a balance of soft interactions—a competition between intrafilm intermolecular forces and substrate/overlayer forces. As a result the effect of substrate on surface orientation is similar in the three types of interfacial systems, but exhibits some differences. Most notable is the tendency of the regular PAH in thin film studies to pack in edge-on herringbone patterns in multilayer films where the molecules do not lie in any single plane and are thus poorly compatible with face-on orientation on lamellar substrates.

Theoretical treatments of anchoring have considered both entropic and energetic effects.[35] Simple entropic considerations favor face-on anchoring for disks[33] because this state minimizes the excluded volume near the interface.[33] This argument implies that in the absence of energetic interactions, the most natural (highest entropy) state for hard disks at a flat interface is to lie parallel (face-on), which is indeed the intuitive result. The simplest theory of energetic interactions is the Creagh−Kmetz rule,[34] which states that a liquid crystal will anchor to place its lower energy surface in contact with low-energy substrates (i.e., those where $\gamma_s < \gamma_l$) and its higher energy surface in contact with high-energy substrates (i.e., those where $\gamma_s > \gamma_l$). [This is the limiting case of the Creagh−Kmetz rule valid when the anisotropic part of the liquid surface tension ($\Delta\gamma_l \equiv \gamma_l^{max}(\theta) - \gamma_l^{max}(\theta)$) is small compared to γ_l.). When applied to carbonaceous mesophase this rule correctly predicts edge-on anchoring (the low γ_l state) on PTFE, but incorrectly predicts face-on anchoring (the high γ_l state) on all the other substrates because they have significantly higher surface energies (67−78 mJ/m^2 in Table 2) than the liquid surface tension (27 mJ/m^2 in Table 2). A new formulation is needed to explain the observed tendency toward edge-on anchoring, as neither entropic considerations[35] nor simple energetic considerations (Creagh−Kmetz rule)[34] predict the correct trend.

Not only the anchoring behavior but also the wetting behavior of the polyaromatic liquids is anomalous in several respects. First, a standard assignment of liquid polarity is often derived by applying the Fowkes theory[44] to the measured surface tension and contact angle on nonpolar PTFE (see Table 2). This calculation involves combining the Young equation (eq 1)

$$\gamma_s = \gamma_{sl} + \gamma_l \cos\theta \tag{1}$$

with the Fowkes equation[44] for dispersive interactions with a nonpolar surface (eq 2)

$$\gamma_{sl} = \gamma_s + \gamma_l - 2(\gamma_s^d \gamma_l^d)^{1/2} \tag{2}$$

to yield eq 3 for the dispersive part of the liquid surface tension, γ_l^d

$$\gamma_l^d = (\gamma_l^2/4\,\gamma_s^d)(1+\cos\theta)^2 \tag{3}$$

The polar part of the liquid surface tension then follows by difference, $\gamma_l^p = \gamma_l - \gamma_l^d$. This standard procedure applied to AR mesophase yields a dispersive component of 20 mJ/m^2 and by difference a polar component of 7.2 mJ/m^2 (26% of the total). This apparent 26% polarity is quite surprising in light of the purely hydrocarbon nature of this liquid (C,H > 99 wt%, O = 0.33 wt%). The same anomaly is also seen to a lesser extent for the smaller aromatic dimethylbenz[*a*]anthracene, $C_{20}H_{16}$, studied here as a model polyaromatic pure compound (26 mJ/m^2 surface tension with an apparent polar component of 2.9 mJ/m^2 or 11.2% polarity) and for A240 isotropic pitch (32.5 mJ/m^2 surface tension with an apparent polar component of 4.8 mJ/m^2 or 14.5% polarity). A further aspect of the anomalous wetting behavior is the increase in AR contact angle as substrate surface energy increases from 65 to 78 mJ/m^2 as shown in Table 2. This increase is quite inconsistent with the notion of a polar component in AR, whose presence would lead to enhanced wetting (decreased contact angle) on substrates of increasingly polarity. Calculations indicate that the temperature dependence of solid surface energies is too weak to account for these wetting anomalies.

(41) White, J. L.; Buecheler, M.; Ng, C. B. *Carbon* **1982**, *20*, 536.
(42) Zimmer, J. E.; White, J. L. In *Advances in Liquid Crystals, Vol. 5*; Academic Press: New York, 1982.
(43) Lewis, R. T.; Bacon, R. *19th Biennial Conference on Carbon;* American Carbon Society, 1989; pp 248−249.
(44) Fowkes, F. M. *Ind. Eng. Chem.* **1964**, *56* (12), 41.

Quantitative treatment of the wetting data set shows it to be inconsistent with the Fowkes,[44] Owens−Wendt,[38] and Van Oss[40] theories of noncovalent interfacial interaction, which each predict complete wetting ($\theta = 0$) of all surfaces except PTFE. Generally, polyaromatic liquids exhibit weaker noncovalent interactions with surfaces than is predicted by the commonly applied interfacial theories, all of which of course were developed from data on nonpolyaromatic liquids. It is clear we must reject the standard assignment of polarity in AR mesophase, and seek an alternate explanation for the raw observation that gives rise to that assignment: a weaker than expected interaction (higher contact angle) with PTFE and with the other substrates as well. For liquid crystals, both experiments[45−47] and models/simulations[48−50] show interaction between wetting behavior and molecular ordering at the interface or in the spreading film. Because the anomalous behavior we report here is a feature of all the polyaromatic liquids studied, regardless of whether they are single-component and whether they form an LC phase upon softening, we seek a more general explanation based on the molecular structure of large PAHs.

A $\pi-\pi$-Bond Theory of Wetting, Anchoring, and Assembly. We propose that both the poor wetting and the favored edge-on anchoring state are the result of relatively strong noncovalent face−face interactions involving aromatic π clouds—so-called "$\pi-\pi$ interactions".[30] Aromatic $\pi-\pi$ interactions are of intense interest for their role in molecular recognition, DNA base-pair interactions, the tertiary structure of proteins, and a host of other phenomena.[30] Critical examination of this literature indicates that in the absence of strongly electron donating or withdrawing groups, $\pi-\pi$ interactions are dominated by dispersion and quadrapolar forces, the latter being responsible for the tilted and offset arrangements in smaller molecules.[30] Charge transfer or orbital overlap affects electrical conductivity in $\pi-\pi$ stacks,[51] but does not typically determine overall energy or configuration in the absence of very strong electron donating or withdrawing groups.[30,52] As molecular size increases, the dispersion forces prevail over the weak quadrapolar forces, producing face-to-face stacking with only slight offset among large molecules, as confirmed experimentally by TEM studies of polyaromatic liquids and young carbon solids.[3]

Our specific explanation for the anomalous wetting and anchoring data is based on the unique geometry of $\pi-\pi$ dispersion interactions as follows. The distinctive structural feature of large polyaromatics is extended molecular planarity, which gives rise to a high area-density of dispersive centers for interaction with adjacent atomic planes. In the case of face-on anchoring, atomic-scale irregularity of most surfaces prevents a large fraction of the carbon atoms from achieving the optimal interatomic distances across the interface, as they would internally through $\pi-\pi$ interaction. This geometric phenomenon can be expected on amorphous solids, real (heterogeneous) surfaces, and even for single crystals except those cleaved along planes of high atomic surface density such as graphite or mica. In the edge-on state, the disk/surface interactions are also limited by the fixed geometry of the solid surface (whether planar or rough), which would rarely conform closely to the circular geometry of the large, edge-on disk. The common application of interfacial theories assumes interatomic spacings across the interface are the same as those within each of the bulk phases, a requirement that is approximately fulfilled for liquids composed of small molecules. For larger molecules the effective dispersion centers are typically redefined as small molecular subunits to preserve the usefulness of the theories in their simple form.[44] This approach fails, however, for large polyaromatics that are insufficiently flexible for subunits to accommodate complex surface topologies.

Here we describe interfacial energies for nonpolar liquids with the classical approach modified by a factor F_I to account for geometric mismatch

$$\gamma_{sl}(\theta) = \gamma_s + \gamma_l(\theta) - 2F_I(\theta)\sqrt{\gamma_s^d\,\gamma_l^d(\theta)} \qquad (4)$$

where γ_s, γ_l, and γ_{sl} are the interfacial energies of the solid, liquid, and interface respectively, the latter two depending on the angle, θ, of the discotic molecular planes from the substrate. The superscript "d" denotes the dispersive component. The inhibition factor, F_I, represents geometric mismatch in the interfacial zone, and its functional form depends on the anchoring state. For edge-on anchored disks F_I can be estimated as

$$F_I = 4(d_{disk}d_{jj-s})/(d_{disk} + d_{jj-s})^2 \quad \text{(for edge-on anchoring)} \qquad (5)$$

by the same reasoning employed in the earlier derivation for spherical molecules of differing size[53] which involves summation of Lennard−Jones pair potentials across the phase boundary for two semi-infinite slabs.[53] Here d_{disk} is the diameter of the disklike polyaromatics and d_{jj-s} is a mean interatomic spacing in the solid phase. For flat, face-on anchored disks F_I is primarily determined by atomic irregularity in the surface layer, which prevents optimal dispersive interactions for some atoms (dispersion centers) in the solid phase. Pairwise summation of the dispersion interactions gives

$$F_I = \frac{\left(\sum\sum U_{ij}(r_{ij})\right)}{\left(\sum\sum U_{ij}(r_{jj})\right)} \quad \text{(for face-on anchoring)} \qquad (6)$$

where U_{ij} is the liquid/surface atomic pair potential, i and j are dispersion centers in the liquid and solid, respectively, and r is the relevant interatomic distance. The top summation evaluates the potential at the interatomic distances across the interface, while the

(45) Xu, L.; Salmeron, M.; Bardon, S. *Phys. Rev. Lett.* **2000**, *84* (7), 1519−1522.
(46) Oh, S. K.; Nakagawa, M.; Ichimuura, K. *J. Mater. Chem.* **2001**, *11* (6), 1563−1569.
(47) Burhanudin, Z.; Etchegoin, P. *Chem. Phys. Lett.* **2001**, *336* (1−2), 7−12.
(48) Emerson, A. P. J.; Faetti, S.; Zannoni, C. *Chem. Phys. Lett.* **1997**, 271(4−6), 241−246.
(49) Mills, S. J.; Care, C. M.; Neal, M. P.; Cleaver, D. J. *Phys. Rev. E* **1998**, *58* (3), 3284−3294.
(50) Rey, A. D. *Mol. Cryst. Liq. Cryst.* **1999**, *333*, 15−23.
(51) Marcek, A. *Carbon* **2000**, *368*, 1863.
(52) Cozzi, F.; Cinquini, M.; Annuziata, R.; Siegel, J. *J. Am. Chem. Soc.* **1993**, *115*, 5330.
(53) Girifalco, L. A.; Good, R. J. *J. Phys. Chem.* **1957**, *61*, 904.

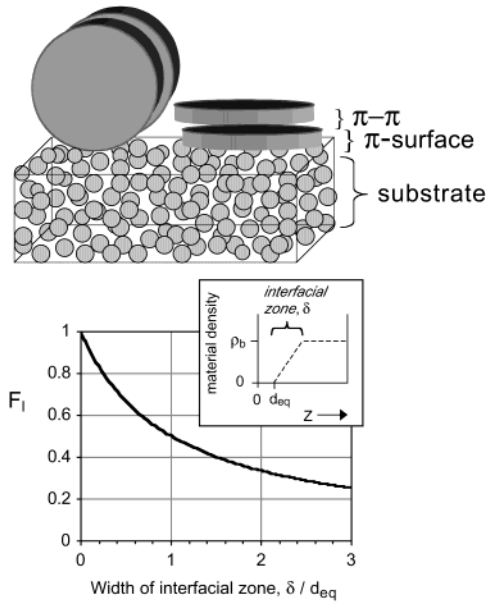

Figure 4. Sketch of noncovalent interaction between large discotic polyaromatics and an amorphous solid phase showing the geometric mismatch responsible for inhibited dispersion. Graph gives inhibition factor, F_I, for face-on disks by eq 7 as a function of the degree of surface irregularity expressed as a width of the interfacial zone. This model calculation assumes linear density profile in the interfacial zone (shown in inset) with the lateral scale of irregularity much smaller than the size of the polyaromatic molecules. Calculation based on the inverse square dependence of Lennard–Jones attractive forces between two infinite slabs.

bottom summation evaluates the potential at interatomic distances characteristic of the solid phase.

Figure 4 shows F_I values computed from eq 6 for one particularly simple model of the interface, in which the material density decreases linearly from its full value to zero over a distance δ, which can be considered the width of an interfacial zone. The calculation considers only attractive forces, which obey an inverse sixth-power dependence on atomic separation distance. For two semi-infinite slabs the net attractive force then follows an inverse square law with separation distance, leading to the following specific model expression for F_I:

$$F_I = U_{ij}/U_{jj} = \int_{r_{jj}}^{r_{jj}+\delta} (r_{jj}/z)^2 \frac{d\rho_o}{dz}\, dz = r_{jj}/\delta - \frac{(r_{jj}/\delta)^2}{(r_{jj}/\delta)+1} \quad (7)$$

where r_{jj} is the interatomic distance in the bulk solid and $(d\rho_o/dz)\, dz$ is the fraction of the solid surface whose closest approach to the nuclei in the first molecular layer is z, which takes the constant value $^1/_\delta$ for the simple linear interface model. Figure 4 shows that the total dispersion energy falls off very sharply with increasing irregularity (increasing δ/r_{jj}), and the inhibition is significant even when the sparse interfacial zone is thinner than one interatomic distance in the bulk solid ($\delta/r_{jj} < 1$). Note that this atomic surface irregularity or "roughness," δ/r_{jj}, is chemical rather than physical in origin and is distinct from the coarser nano- or microscale roughness often characterized by atomic force microscopy.

Combining eq 4 with the Young equation (eq 1) allows F_I values to be calculated from the measured contact angles, surface tension, and substrate surface energies as follows:

$$F_I = (1/2)\,(1 + \cos\theta)(\gamma_s^d/\gamma_l^d)^{0.5} \quad (8)$$

Assuming the polyaromatics to be strictly nonpolar ($\gamma_l^d = \gamma_l$, the total measured surface tension), F_I values are calculated to range from 0.79 to 0.86 (see Table 2), implying reasonable values of 2.7–2.2 for the ratio of disk size to interatomic spacing by eq 5.

This inhibited dispersion phenomenon provides an explanation for the edge-on anchoring trend as follows. The preferred anchoring state corresponds to the angle, θ, that gives the minimum interfacial free energy, $\gamma_{sl}(\theta)$, in eq 4. If we assume for simplicity that F_I is similar in face-on and edge-on configuration, and that the anisotropic part of the liquid surface tension ($\Delta\gamma_l \equiv \gamma_l^{max}(\theta) - \gamma_l^{max}(\theta)$) is small, the following particularly simple and insightful criterion is derived by minimization of $\gamma_{sl}(\theta)$: If $F_I^2\gamma_s^d > \gamma_l$, then interfacial energy effects favor face-on anchoring, and if $F_I^2\gamma_s^d < \gamma_l$, then interfacial energies favor edge-on anchoring. The criterion introduces the quantity $F_I^2\gamma_s^d$ as an effective solid surface energy for the inhibited dispersion interaction with large rigid, nonpolar molecular disks. Substitution of F_I and γ_l^d values from Table 2 into this criterion clearly shows the energetic preference of edge-on anchoring, $F_I^2\gamma_s^d$, is always less than γ_l. In physical terms, inhibition makes π-surface interactions weaker than internal π–π interactions, even for the highest energy substrates investigated. The two exceptions to the edge-on trend are the lamellar materials graphites and mica, which have among the highest values of $F_I^2\gamma_s^d$, though still slightly less than the AR surface tension. This simple theory based on the effective dispersion energy, $F_I^2\gamma_s^d$, captures the major trends, but is not fully predictive, and could be extended to include both finite $\Delta\gamma_l$ and explicit treatment of entropic effects on anchoring.

A direct consequence of the present results is that internal π–π bonds in polyaromatic liquids will be stronger than π–non-π surface bonds in most cases, and polyaromatics will assemble in a way that preserves π–π bonding—a simple rule with the power to explain many observed phenomena, including: (1) the early formation of local π–π columnar structures within natural polyaromatic mixtures,[3] (2) the strong adsorption of aromatics on carbonaceous sorbents,[54] which offer strong π–π surface interaction, (3) the high affinity of aromatic solvents for chromatographic packings that incorporate aromatic functionality,[55] (4) the preference for edge-on anchoring observed here, which preserves internal π–π bonds at the expense of potential π–surface bonds (the exceptions are the atomically flat lamellar materials graphite and mica that offer strong dispersive interactions with π systems that can successfully compete with internal π–π bonds), and (5) the "inverted" structure of Brooks–Taylor carbon spheres reported in *Nature*[5] in 1965 (see below). Finally, our inability to order these discotic interfaces in-plane with

(54) Radovic, L. R.; Moreno-Castilla, C.; Rivera-Utrilla, J. In *Chemistry and Physics of Carbon, Vol 27*; Marcel Dekker: New York, 2001.

(55) Leon, J.; Reubsaet, E.; Vieskar, R. *J. Chromatogr. A* **1999**, *841*, 147.

directional rubbing may also be a reflection of the relatively weak edge-on interfacial interactions relative to liquid/liquid intermolecular forces dominated by $\pi-\pi$ interaction.

Structure Selection in Carbon Materials. The origin of the inverted bipolar configuration of Brooks–Taylor carbon spheres (Figure 1) may now be understood as follows. During heating of the complex organic precursor mixture, polymerization and vaporization of small molecules allows the larger disklike polyaromatics to spontaneously assemble in face-to-face mode to form an orientationally ordered fluid that maximizes $\pi-\pi$ bonding. This $\pi-\pi$ interaction is further enhanced by expelling small or defective weak-π-bond-formers to a surrounding isotropic phase. Within the droplets of the high-molecular-weight ordered fluid, the particular bipolar configuration arises as a requirement of edge-on surface anchoring, selected by the same underlying rule: it preserves internal $\pi-\pi$ bonds at the expense of the weaker potential π bonds with the surrounding disordered liquid. Indeed the observed bipolar structure achieves all possible internal $\pi-\pi$ interactions except for two point defects at the polar caps (see Figure 1), and is thus favored over the alternative, symmetry-allowed concentric, "onion" structure (see Figure 1), which would sacrifice a full set of internal $\pi-\pi$ bonds at the periphery.

We are now in a position to summarize the underlying assembly rules leading to open and closed carbon forms. Closed carbon forms (nanotubes, fullerenes, carbon black, soot, and pyrolytic carbon films) are synthesized at high temperature along chemical pathways that attempt to minimize high-energy edge sites with unsaturated valencies. The resulting structures contain few or no unsatisfied edge-sites and their exposed surfaces are rich in basal plane carbon. In contrast, the open forms are synthesized at a lower temperature where edge-site valencies are satisfied by hydrogen and chemical reactivity is low. At the same time noncovalent $\pi-\pi$ forces are significant relative to kT, and cause a "face-to-face assembly" process under essentially chemically frozen conditions. That assembly expels the H-saturated, low-energy edge sites to the periphery of the structure to achieve the preferred edge-on anchoring state and preserve $\pi-\pi$ bonds. Once these edge-on domains form, wholesale rearrangement to face-on structures can be difficult, and further heating often brings about polymerization of the domain structure to produce "inverted" carbon materials with all-edge surfaces.

These results open new possibilities for the molecular design of carbons. Using Table 1 as a guideline for selecting anchoring templates we have demonstrated the ability to imprint spatial patterns of discotic molecular orientation on surfaces. Figure 5 shows a periodic microarray of edge-on and face-on surface regions produced using a Cu/HOPG two-component anchoring template. Such textured surfaces have been prepared in the raw polyaromatic solids and also in fully carbonized materials obtained by oxidative stabilization of the ordered polyaromatic thin films when they are thin (<50 μm) at around 200 °C followed by heat treatment above 700 °C. The synthesis of a variety of new carbon forms can be envisioned by this principle including nanoscale all-edge carbons made using three-dimensional nanoporous templates. Because many important carbon properties are highly sensitive to graphene layer orientation, such systematic molecular engineering of orientational patterns has long been a key goal of carbon science.

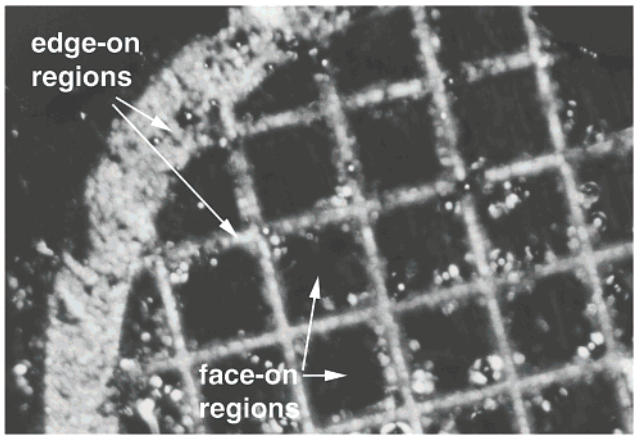

Figure 5. Optical micrograph (crossed polars) showing polyaromatic solid surface with microscale molecular orientational pattern established with a two-component surface anchoring template. The template was a Cu TEM grid (imparting edge-on anchoring) on a cleaved HOPG graphite basal surface (imparting face-on anchoring). After physical removal of the template, the grid pattern is clearly evident as bright anisotropic (edge-on) regions at the former Cu interface and dark isotropic (face-on) regions at the former graphite interface. It is anticipated that a variety of new carbon forms with programmed graphene layer orientations can be synthesized by this principle.

Acknowledgment. Funding from the ACS Petroleum Research Fund, the National Science Foundation, the U.S. Department of Energy, and the Fulbright Program (G.K.) are gratefully acknowledged. We also acknowledge sample donation by Mitsubishi Gas Chemical and Profs. D. Edie and M. Thies at Clemson University, and Ashland Oil Company. We are grateful for technical discussions with Dr. Christopher Hunter at Sheffield University on $\pi-\pi$ bonding, and for the use of facilities at the University of Sydney, New South Wales, provided by Prof. Brian Haynes.

CM020310B